

**STRUCTURAL AND OPTOELECTRONIC CHARACTERISATIONS OF
ZINC OXIDE STRUCTURES FOR ANTIBACTERIAL
ACTIVITIES ON SKIN BACTERIA**

LING CHUO ANN

UNIVERSITI SAINS MALAYSIA

2014

**STRUCTURAL AND OPTOELECTRONIC CHARACTERISATIONS OF
ZINC OXIDE STRUCTURES FOR ANTIBACTERIAL ACTIVITIES ON
SKIN BACTERIA**

By

LING CHUO ANN

**Thesis submitted in fulfillment of the requirements for the degree of Doctor of
Philosophy**

September 2014

ACKNOWLEDGEMENT

At the moment when I finished completing my thesis, many people who have contributed to my work and helped me in the life came into my mind. Sincerely, I appreciate and cherish everything that has done for me. Firstly, I would like to express my deepest gratitude to my main supervisor Dr. Shahrom Mahmud for his guide and tutor in the whole research work. With your immense knowledge, you help me open the mind to learn and look into the physics world. It is my honor to be your student and I am proud of it. I also would like to thank my co-supervisors Dr. Habsah Hasan, Dr. Dasmawati Mohamad and Dr. Md Azman Seeni Mohamed for their guide, help and support in succeeding the antibacterial and cytotoxicity's tests. They provided and shared their research laboratories (microbiology lab and toxicology lab) to our group to conduct the antibacterial and cytotoxicity's test. Besides, they also taught and guided me on the experimental work. The biological works were new experiences and knowledge which beyond my physics' background. I would like to extend my gratitude to the staff in Nano-optoelectronics Research (NOR), Technology Laboratory, electron microscopy (EM) laboratory, microbiology laboratory Kelantan and toxicology laboratory IPPT for their technical assistance and valuable contribution to my work. In addition, my appreciation also goes to the research group members Siti Khadijah Mohd Bakhori and Amna Sirelkhatim for their helps in the experimental works. Last but not least, special thanks to my parents who always accompanied and encouraged me in the last three and half years. Thank you so much.

Ling Chuo Ann

Pulau Pinang, Malaysia. March 2014

TABLE OF CONTENTS

CONTENTS	PAGES
ACKNOWLEDGEMENT	ii
TABLE OF CONTENTS	iii
LIST OF FIGURES	viii
LIST OF TABLES	xii
LIST OF SYMBOLS	xiii
LIST OF ABBREVIATIONS	xv
ABSTRAK	xvii
ABSTRACT	xix
CHAPTER 1: INTRODUCTION	
1.1 Nanomaterials	1
1.2 ZnO powder	2
1.3 Skin bacteria	4
1.4 Fibroblast cell lines	6
1.5 Objectives of study	6
1.6 Scope of study	7
1.7 Design of experiment	9
1.8 Background of study	10
1.9 Overview of study	12
CHAPTER 2: LITERATURE REVIEW	
2.1 Introduction	15
2.2 Application of zinc oxide	15
2.3 Properties of zinc oxide	16

2.4	Electrical property of ZnO	18
2.5	Optical property of ZnO	19
2.5.1	Non-radiative via deep level energy	23
2.5.2	Auger recombination	24
2.5.3	Surface recombination	25
2.6	Skin bacteria	27
2.6.1	<i>Staphylococcus aureus</i>	28
2.6.2	<i>Streptococcus pyogenes</i>	28
2.6.3	<i>Pseudomonas aeruginosa</i>	29
2.7	Bacteria structure	30
2.7.1	Gram-positive bacteria	31
2.7.2	Gram-negative bacteria	32
2.8	Antibacterial activity of zinc oxide	33
2.9	Toxicity of ZnO particles	35
2.10	Reactive oxygen species	37
2.11	Fibroblast cell lines	38
2.12	Calamine lotion	38

CHAPTER 3: METHODOLOGY

3.1	Introduction	40
3.2	Synthesis of ZnO	40
3.3	Annealing treatment of ZnO	41
3.4	Electron microscopy	42
3.4.1	Electron spectroscopy imaging	44
3.4.2	Transmission electron microscopy	46

3.4.3	Field-emission scanning electron microscopy	48
3.5	Current-voltage measurement	50
3.6	X-ray diffraction	52
3.7	Thermogravimetric analysis	55
3.8	Optical property measurements	56
3.8.1	Photoluminescence	56
3.8.2	Raman spectroscopy	59
3.8.3	UV-Visible spectroscopy	61
3.9	Antibacterial study	63
3.10	Cytotoxicity test of ZnO-Pharma and ZnO-White	67
3.11	Calamine lotion preparation	69
3.12	Antibacterial test of calamine lotion	70

CHAPTER 4: EXPERIMENTAL RESULTS

4.1	Introduction	72
4.2	Morphological and elemental mapping analysis	72
4.3	X-ray diffraction analysis	79
4.4	Electrical measurement	83
4.5	Thermogravimetric analysis	89
4.6	Photoluminescence	90
4.7	Optical absorption	94
4.8	Raman spectroscopy	95
4.9	Antibacterial properties	97
4.9.1	<i>Staphylococcus aureus</i>	97
4.9.2	<i>Pseudomonas aeruginosa</i>	99

4.9.3	<i>Streptococcus pyogenes</i>	101
4.9.4	Percentage inhibition after 24 h	103
4.10	Effect of surface medication and UVA excitation	105
4.11	Cytotoxicity of ZnO on L929 fibroblasts cell lines	109
4.12	Antibacterial responses of calamine lotions	113

CHAPTER 5: ANALYSIS AND DISCUSSIONS

5.1	Introduction	118
5.2	Key factors of antibacterial	118
5.3	Proposed mechanisms of antibacterial activity	121
5.3.1	<i>Staphylococcus aureus</i>	122
5.3.2	<i>Pseudomonas aeruginosa</i>	124
5.3.3	<i>Streptococcus pyogenes</i>	125
5.4	Effect of surface modification on antibacterial property	126
5.5	Effect of UVA illumination on antibacterial property	130
5.6	Potential application of ZnO in calamine lotion	131
5.6.1	Cytotoxicity of ZnO	131
5.6.2	Antibacterial application of calamine lotions	134

CHAPTER 6: CONCLUSIONS AND FUTURE DIRECTIONS

6.1	Conclusions	136
6.2	Future research direction	139

REFERENCES	141
-------------------	-----

APPENDICES

Appendix A	158
Appendix B	159
Appendix C	160
Appendix D	162
LIST OF PUBLICATIONS	164

LIST OF FIGURES

		Pages
Figure 1.1	Annual production volumes of nanomaterials	2
Figure 1.2	Flow chart of experiment	9
Figure 2.1	Hexagonal wurtzite-type lattice of ZnO crystal structure	16
Figure 2.2	(a) Radiative recombination; (b) Non-radiative recombination	22
Figure 2.3	Band transitions in a semiconductor: (a) non-radiative via deep level; (b) non-radiative via Auger process; (c) radiative with a photon emission.	23
Figure 2.4	Energy levels of native defects in ZnO	24
Figure 2.5	(a) Band-bending caused by Fermi level pinning at the surface; (b) Steady-state excess hole concentration versus distance from a semiconductor surface.	26
Figure 2.6	Skin infections on a human being	29
Figure 2.7	Morphology of a bacterial cell	30
Figure 2.8	The envelope of gram-positive bacteria	32
Figure 2.9	The envelope of gram-negative bacteria	33
Figure 2.10	Toxic effect of ZnO particles	37
Figure 3.1	LENTON VTF/12/60/700 annealing tube furnace	42
Figure 3.2	Electron-specimen interactions and secondary effects	43
Figure 3.3	(a) Instrumentation of EFTEM-ESI; (b) Zeiss Libra 120 EFTEM	45
Figure 3.4	(a) Instrumentation of TEM; (b) Philips CM12 TEM	47
Figure 3.5	(a) Instrumentation of FESEM; (b) FEI Nova NanoSEM 450 FESEM	49
Figure 3.6	(a-b) Keithley 4200-SCS current-voltage	51
Figure 3.7	(a) Connection of electrical probes on a ZnO pellet surface; (b) UVA exposed on ZnO pellet; (c) wavelength spectrum of UVA light	51

Figure 3.8	X-ray diffraction on crystals lattice	53
Figure 3.9	(a) Panalytical X'pert Pro Mrd Pw3040 X-ray diffractometer; (b) Instrumentation of XRD	54
Figure 3.10	Mettler Toledo SDTA851 Thermogravimetric analysis	56
Figure 3.11	(a) Jobin Yvon Horiba HR800UV photoluminescence; (b) Instrumentation of photoluminescence	58
Figure 3.12	Transition mechanism of Raman scattering	59
Figure 3.13	Typical Raman spectroscopy	60
Figure 3.14	(a) Shimadzu 1800 UV-Visible spectrophotometer; (b) Instrumentation of UV-Visible	62
Figure 3.15	Subculture of (a) <i>S. aureus</i> and (b) <i>S. pyogenes</i>	64
Figure 3.16	(a) Bacteria treated with ZnO in a 96-well plate; (b) UVA 68 illumination on the bacteria and ZnO mixture	65
Figure 3.17	BP, Essentiel, ZnO-Pharma and ZnO-White calamine lotions	70
Figure 4.1	FESEM and EDS images of (a) ZnO-Pharma and (b) ZnO-White	73
Figure 4.2	TEM images and particle distribution of: (a-b) ZnO-Pharma; (c-d) ZnO-White	74
Figure 4.3	TEM images of ZnO-Pharma: (a) unannealed; (b) N ₂ annealed and (c) O ₂ annealed ZnO-Pharma; ZnO-White: (d) unannealed; (e) N ₂ annealed and (f) O ₂ annealed	75
Figure 4.4	ESI mapping of ZnO-Pharma: (a) Unannealed; (b) N ₂ annealed; (c) O ₂ annealed	76
Figure 4.5	ESI mapping of ZnO-White: (a) unannealed; (b) N ₂ annealed; (c) O ₂ annealed	78
Figure 4.6	XRD spectra of: (a) ZnO-Pharma and (b) ZnO-White	79
Figure 4.7	Current-voltage measurement of: (a) ZnO-Pharma and (b) ZnO-White	84
Figure 4.8	Schematic diagram representation of the surface band bending of ZnO at two different stages: (a) O ₂ annealed and (b) N ₂ annealed; l =depletion layer thickness; $V(x)$ = surface potential; x = distance from the surface	86

Figure 4.9	UVA photo-response of: (a) ZnO-Pharma pellet; (b) ZnO-White pellet	87
Figure 4.10	(a) UV excitation mechanism on ZnO pellet surface; (b) Energy band diagram of ZnO under UV excitation	89
Figure 4.11	TGA curves of ZnO-Pharma and ZnO-White	90
Figure 4.12	Photoluminescence spectra of (a) ZnO-Pharma and (b) ZnO-White	92
Figure 4.13	Optical absorption of (a) ZnO-Pharma powder; (b) ZnO-White powder	95
Figure 4.14	Raman spectra of (a) ZnO-Pharma and (b) ZnO-White	96
Figure 4.15	FESEM images of (a) untreated <i>S. aureus</i> and (c) treated <i>S. aureus</i> ; EDS spectra of (b) untreated <i>S. aureus</i> and (d) treated <i>S. aureus</i>	98
Figure 4.16	OD measurement of <i>S. aureus</i> growth using different concentration of (a) ZnO-Pharma and (b) ZnO-White	99
Figure 4.17	FESEM images of (a) untreated <i>P. aeruginosa</i> and (c) treated <i>P. aeruginosa</i> ; EDS spectra of (b) untreated <i>P. aeruginosa</i> and (d) treated <i>P. aeruginosa</i>	100
Figure 4.18	OD measurement of <i>P. aeruginosa</i> growth using different concentration of (a) ZnO-Pharma and (b) ZnO-White	101
Figure 4.19	FESEM images of (a) untreated <i>S. pyogenes</i> and (c) treated <i>S. pyogenes</i> ; EDS spectra of (b) untreated <i>S. pyogenes</i> and (d) treated <i>S. pyogenes</i>	102
Figure 4.20	OD measurement of <i>S. pyogenes</i> growth using different concentration of (a) ZnO-Pharma and (b) ZnO-White	103
Figure 4.21	Percentage inhibition of <i>S. aureus</i> , <i>P. aeruginosa</i> and <i>S. pyogenes</i> treated with 2 mM of ZnO-Pharma and ZnO-White respectively.	104
Figure 4.22	OD measurement of <i>S. aureus</i> being treated with (a) ZnO-Pharma and (b) ZnO-White.	106
Figure 4.23	OD measurement of <i>P. aeruginosa</i> being treated with (a) ZnO-Pharma and (b) ZnO-White.	107
Figure 4.24	Percentage inhibition of (a) <i>S. aureus</i> and (b) <i>P. aeruginosa</i> being treated with ZnO-Pharma and ZnO-White after 24 h.	108

Figure 4.25	Morphologies of <i>L929</i> cell lines after being treated with different concentration of ZnO-Pharma: (a) Control, (b) 0.1mM, (c) 0.2mM, (d) 0.3mM, (e) 0.4mM and (f) 0.5mM	110
Figure 4.26	Morphologies of <i>L929</i> cell lines after being treated with different concentration of ZnO-White: (a) Control, (b) 0.1mM, (c) 0.2mM, (d) 0.3mM, (e) 0.4mM and (f) 0.5mM	111
Figure 4.27	Percentage of viable cells of <i>L929</i> fibroblast treated with different concentration of ZnO-Pharma and ZnO-White.	112
Figure 4.28	Colony counts of <i>S. aureus</i> [(a) ZnO-Pharma calamine lotion and (b) ZnO-White calamine lotion]; <i>P. aeruginosa</i> [(c) ZnO-Pharma calamine lotion and (d) ZnO-White calamine lotion]; <i>S. pyogenes</i> [(e) ZnO-Pharma calamine lotion and (f) ZnO-White calamine lotion].	114
Figure 4.29	Colony counts of (a) <i>S. aureus</i> , (b) <i>P. aeruginosa</i> and (c) <i>S. pyogenes</i> after being treated with calamine lotions.	115
Figure 5.1	Schematic diagram of ZnO particles' characteristics	119
Figure 5.2	Schematic diagram of the generation of O_2^- , $\bullet OH$ and H_2O_2	129

LIST OF TABLES

		Pages
Table 2.1	Typical properties of ZnO	17
Table 2.2	Optical phonon modes of ZnO bulk and thin films samples through Raman spectroscopy	21
Table 2.3	Common bacterial structures and their functions	31
Table 2.4	Electron structures of common reactive oxygen species	37
Table 3.1	Formulation of calamine lotion	69
Table 4.1	Structural parameters of ZnO annealed under different ambient at 700°C	82
Table 4.2	Raman modes observed from ZnO-Pharma and ZnO-White	97
Table 4.3	Percentage inhibitions of bacteria treated with BP, Essentiel, ZnO-Pharma and ZnO-White calamine lotions	116

LIST OF SYMBOLS

a	Basal plane lattice constant
c	Uniaxial lattice constant
u	Internal coordinate
hkl	Miller indices
T	Absolute temperature
C_p	Specific heat capacity
m_0	Electron mass
Γ	Wurtzite-structure optical phonons
ω	Phonon frequency
R_s	Recombination rate
p	Hole concentration
τ	Lifetime
D_p	Diffusion coefficient
s	Surface recombination velocity
O_2^-	Superoxide anion
H_2O_2	Hydrogen peroxide
$\bullet OH$	Hydroxyl radical
E	Energy
h	Planck's constant
c	Speed of light
λ	Wavelength
d	Lattice plane distance
n	Integer
θ	Scattering angle

ν	Frequency
t	Grain sizes
I	Intensity of beam
A	Absorbance
b	Path length
e	Molar absorbtivity
x	Concentration
n	Statistical n-trial
p	Statistical p -value
ε_z	Strain
σ	Stress
C	Elastic stiffness constants
G	Surface conductance
e	Electron
I	Current
V	Voltage

LIST OF ABBREVIATIONS

ZnO	Zinc oxide
eV	Electron volt
UV	Ultraviolet
UVA	Ultraviolet-A
PL	Photoluminescence
TEM	Transmission electron microscope
FESEM	Field-emission scanning electron microscope
EFTEM	Energy-filtering transmission electron microscope
ESI	Electron spectroscopy imaging
EDS	Energy dispersive spectroscopy
TGA	Thermogravimetric analysis
XRD	X-ray diffraction
O	Oxygen
Zn	Zinc
ROS	Reactive oxygen species
TO	Transverse optical
LO	Longitudinal optical
V _o	Oxygen vacancy
Zn _i	Zinc interstitial
E _v	Valence band
E _c	Conduction band
<i>S. aureus</i>	<i>Staphylococcus aureus</i>
<i>P. aeruginosa</i>	<i>Pseudomonas aeruginosa</i>
<i>S. pyogenes</i>	<i>Streptococcus pyogenes</i>

LPS	Lipopolysaccharides
FWHM	Full-wave half maximum
NBE	Near-band-edge
GL	Green luminescence
OD	Optical density
SD	Standard deviation

**PENCIRIAN STRUKTUR DAN OPTOELEKTRONIK STRUKTUR ZINK
OKSIDA UNTUK AKTIVITI ANTIBAKTERIA TERHADAP BAKTERIA
KULIT**

ABSTRAK

Objektif utama penyelidikan ini ialah untuk menyiasat sifat struktur dan optoelektronik struktur zink oksida (ZnO) serta perkaitannya dengan aktiviti antibakteria terhadap *Staphylococcus aureus* (*S. aureus*), *Pseudomonas aeruginosa* (*P. aeruginosa*) dan *Streptococcus pyogenes* (*S. pyogenes*). Dua sampel serbuk ZnO, dengan serbuk pertama mempunyai struktur bentuk rod (ZnO-Pharma) manakala serbuk kedua mempunyai bentuk plat (ZnO-White), telah dicirikan dengan sifat morfologi, struktur, optik dan elektrik. Struktur rod mempunyai diameter 30-120 nm dan struktur plat mempunyai ketebalan 40-200 nm. Kajian dengan elektron pengimbasan mendapati perbezaan dalam taburan atom oksigen dan atom zink di atas struktur ZnO, iaitu lebih tinggi nisbah O:Zn bagi struktur rod manakala lebih rendah nisbah O:Zn bagi struktur plat. Dengan menggunakan suhu penyepuhlandapan 700°C, penyepuhlandapan oxygen menyebabkan penjerapan oksigen yang tinggi di atas permukaan struktur ZnO manakala penyepuhlandapan nitrogen menyebabkan penyaherapan oksigen di atas permukaan struktur ZnO. Keputusan kefotopendarcahayaan menunjukkan pancaran hijau yang lebih tinggi daripada permukaan ZnO bawah penyepuhlandapan nitrogen tetapi penyepuhlandapan oksigen menunjukkan kesan sebaliknya terhadap pancaran hijau. Disebabkan penjerapan dan penyaherapan oksigen, penyepuhlandapan nitrogen meningkatkan konduksian permukaan sebanyak lebih kurang 60% manakala penyepuhlandapan oksigen mengurangkan konduksian permukaan sebanyak lebih

kurang 80%. Pencahayaan UVA didapati mempertingkatkan konduksian permukaan dengan nyata sekali, iaitu 6 kali ganda berbanding dengan ZnO yang tidak terdedah.

Sebaliknya, greak balas antibakteria struktur ZnO telah dikaji terhadap *S. aureus*, *P. aeruginosa* dan *S. pyogenes*. Sampel ZnO-Pharma dan ZnO-White menunjukkan penyekatan yang baik terhadap *S. pyogenes* dengan peratus penyekatan lebih daripada 95%. Fenomena ini adalah mungkin disebabkan oleh ketiadaan katalase, menjadikan bakteria mudah diserang oleh spesis oksigen reaktif bertoksik yang dilepaskan oleh ZnO. ZnO-Pharma menyebabkan penyekatan yang lebih tinggi terhadap *S. aureus* dan *P. aeruginosa* berbanding dengan ZnO-White kerana saiz zarah struktur rod yang lebih kecil berbanding dengan struktur plat. Keputusan antibakteria menunjukkan ZnO penyepuhlindungan oxygen menunjukkan penyekatan pertumbuhan yang lebih tinggi sedikit terhadap *S. aureus* dan *P. aeruginosa* berbanding dengan ZnO tanpa penyepuhlindungan. Pencahayaan UVA di atas ZnO menyebabkan penyekatan yang paling tinggi terhadap bakteria di mana penyekatan *S. aureus* bertambah sebanyak 9% (ZnO-Pharma) dan 15% (ZnO-White) manakala penyekatan *P. aeruginosa* bertambah sebanyak 48% (ZnO-Pharma) dan 32% (ZnO-White). Penambahan antibakteria oleh penyepuhlindungan oksigen dan pencahayaan UVA adalah mungkin disebabkan oleh spesis oksigen reaktif yang diaktifkan di dalam ampaiian ZnO. Aras toksikologi sampel ZnO-Pharma dan ZnO-White telah ditentukan kurang daripada 0.3 mM berdasarkan ujian kesitotoksikan terhadap sel fibroblas tikus L929. Losen kalamini ZnO-Pharma dan ZnO-White telah berjaya disediakan, yang menunjukkan greak balas antibakteria yang luar biasa terhadap tiga bakteria kulit.

**STRUCTURAL AND OPTOELECTRONIC CHARACTERISATIONS OF
ZINC OXIDE STRUCTURES FOR ANTIBACTERIAL ACTIVITIES ON
SKIN BACTERIA**

ABSTRACT

The main objective for this research work is to investigate the structural and optoelectronic properties of zinc oxide (ZnO) structures with their correlation on antibacterial activities against *Staphylococcus aureus* (*S. aureus*), *Pseudomonas aeruginosa* (*P. aeruginosa*) and *Streptococcus pyogenes* (*S. pyogenes*). Two ZnO powder samples, one with rod-like (ZnO-Pharma) and the other with plate-like (ZnO-White) structures, were characterised for their morphological, structural, optical and electrical properties. The rods structures were 30-120 nm in diameter and the plates structures were 40-200 nm thick. Electron spectroscopy imaging showed the different distribution of oxygen and zinc atom on the ZnO structures, that is higher O:Zn ratio on rods structures while lower O:Zn ratio on plates structures. Using annealing temperature of 700°C, oxygen annealing induced high oxygen adsorption on ZnO structures surface while nitrogen annealing caused oxygen desorption on ZnO structures surface. The photoluminescence results revealed higher green emission from ZnO surface under nitrogen annealing but the oxygen annealing exhibited adverse effect on green emission. Due to the adsorption and desorption of oxygen, nitrogen annealing improved the surface conductance by about 60% while oxygen annealing decreased the surface conductance by about 80%. UVA illumination was found to enhance the surface conductance significantly, up to 6 times compared to non-exposure ZnO.

On the other hand, antibacterial responses of ZnO structures were studied towards *S. aureus*, *P. aeruginosa* and *S. pyogenes*. ZnO-Pharma and ZnO-White

samples exhibited excellent inhibition towards *S. pyogenes* with the percentage inhibition above 95%. This phenomenon was probably due to the absence of catalase, making the bacteria vulnerable to the toxic reactive oxygen species (ROS) released by ZnO. ZnO-Pharma induced higher inhibition toward *S. aureus* and *P. aeruginosa* than that of ZnO-White because of the smaller particle size of rod structures compared to plate structures. The antibacterial results showed that oxygen-treated ZnO exhibited slightly higher growth inhibition on *S. aureus* and *P. aeruginosa* compared with unannealed ZnO. UVA illumination on ZnO causes the greatest inhibition toward the bacteria where the inhibition of *S. aureus* increased by 9% (ZnO-Pharma) and 15% (ZnO-White) while inhibition of *P. aeruginosa* increased by 48% (ZnO-Pharma) and 32% (ZnO-White). Antibacterial enhancement by oxygen annealing and UVA illumination was probably due to the activated release of reactive oxygen species in ZnO suspension. The toxicology level of ZnO-Pharma and ZnO-White samples was determined to be less than 0.3 mM from the cytotoxicity test on *L929* mouse fibroblast cell lines. ZnO-Pharma and ZnO-White calamine lotions were successfully prepared, which showed remarkable antibacterial response toward three skin bacteria.

LIST OF PUBLICATIONS

Publications

- [1] **L.C.Ann**, S.Mahmud, S.K.M.Bakhori, Electron spectroscopy imaging and surface defect configuration of zinc oxide nanostructures under different annealing ambient, *Applied Surface Science* 265 (2013) 137-144.
- [2] **L.C.Ann**, S.Mahmud, S.K.M.Bakhori, A.Sirelkhatim, D.Mohamad, H.Hasan, A.Seeni, R.A.Rahman, Antibacterial responses of zinc oxide structures against *Staphylococcus aureus*, *Pseudomonas aeruginosa* and *Streptococcus pyogenes*, *Ceramics International* 40 (2014) 2993-3001.
- [3] **L.C.Ann**, S.Mahmud, S.K.M.Bakhori, A.Sirelkhatim, D.Mohamad, H.Hasan, A.Seeni, R.A.Rahman, Effect of surface modification and UVA photoactivation on antibacterial bioactivity of zinc oxide powder, *Applied Surface Science* 292 (2014) 405-412.
- [4] **L.C.Ann**, S.Mahmud, S.K.M.Bakhori, Effects of annealing treatment on photoluminescence and structural properties of ZnO nanostructures, *Advanced Material Research* 501 (2012) 184-188.
- [5] **L.C.Ann**, S.Mahmud, S.K.M.Bakhori, A.Sirelkhatim, D.Mohamad, H.Hasan, A.Seeni, R.A.Rahman, Optical properties and antibacterial bioactivity of ZnO nanopowder annealed in different ambient, *Advanced Material Research* 626 (2013) 324-328.
- [6] **L.C.Ann**, S.Mahmud, S.K.M.Bakhori, A.Sirelkhatim, D.Mohamad, H.Hasan, A.Seeni, R.A.Rahman, Characterization of ZnO nanopowder and antibacterial response against *Staphylococcus aureus* under UVA illumination, *Advanced Material Research* 795 (2013) 148-152.

Conferences

1. **L.C.Ann**, S.Mahmud, S.K.M.Bakhori, Effects of annealing treatment on photoluminescence and structural properties of ZnO nanostructures, 26th Regional Conference on Solid State Science and Technology (RCSSST26). Negeri Sembilan, Malaysia, 22-24 November 2011.
2. **L.C.Ann**, S.Mahmud, S.K.M.Bakhori, A.Sirelkhatim, D.Mohamad, H.Hasan, A.Seeni, R.A.Rahman, Optical properties and antibacterial bioactivity of ZnO nanopowder annealed in different ambient, International Conference on Advanced Material Engineering and Technology (ICAMET 2012). Pulau Pinang, Malaysia, 28-30 November 2012.
3. **L.C.Ann**, S.Mahmud, S.K.M.Bakhori, A.Sirelkhatim, D.Mohamad, H.Hasan, A.Seeni, R.A.Rahman, Characterization of ZnO nanopowder and antibacterial response against *Staphylococcus aureus* under UVA illumination, International

Conference on Sustainable Materials Engineering (ICoSM 2013). Pulau Pinang, Malaysia, 26-27 March 2013.

4. **L.C.Ann**, S.Mahmud, S.K.M.Bakhori, A.Sirelkhatim, D.Mohamad, H.Hasan, A.Seeni, R.A.Rahman, Enhanced photoconductivity and antibacterial response of rubber-grade ZnO upon UVA illumination, Joint International Conference on Nanoscience, Engineering, and Management (BOND 21). Pulau Pinang, Malaysia, 19-21 August 2013.
5. **L.C.Ann**, S.Mahmud, S.K.M.Bakhori, A.Sirelkhatim, Photoconductivity of pharma-grade ZnO under UVA and white light exposure, 27th Regional Conference on Solid State Science and Technology (RCSST27). Kota Kinabalu, Sabah, Malaysia, 20-22 December 2013.

CHAPTER 1: INTRODUCTION

1.1 Nanomaterials

Nanoindustry is one of the fastest developing industries and it has been denoted as the next industrial revolution [1]. Consequently, the global socioeconomic value of nanotechnologies is progressively increasing [2]. Estimated global production of nanoparticles is illustrated in Fig. 1.1 (Piccinno *et al.* [3]). Currently, nanomaterials provide significant impacts on most of the industries and all areas of society. In consumer products, nanoparticles are either added to the bulk material to reinforce the physical properties of the material or applied on the surface of the product to provide enhanced surface features such as scratch resistance, water repellency, reflectivity, photo activity and antimicrobial.

Nanomaterials refer to the substances having at least one critical dimension with nanometric scale below than 100 nm [4]. They have attracted much attention for their unique properties and promising performance compared to macroscopic materials. Nanotechnology has been used as an advanced approach of synthesis and modification of nanomaterials, aiming to obtain improved physical, chemical, electrical, thermal, mechanical, biological properties and functionalities due to their nanoscaled size [4-5]. These unique properties are required for materials' utilization in electronics, energy, medical, engineering and environmental areas. With the development of nanotechnology, a diverse range of nanomaterials are emerging. For example, nanomaterials are present in sunscreens, creams, toothpastes, textile, fibre coatings, catalysts, fuel additives, biosensing, microelectronics, solar cells, electroluminescent devices, cosmetics, detergent and antimicrobials [6-11].

Even though there are numerous current and future applications, the potential impact of nanomaterials on human and environment remain unclear. The behavior of bulk materials cannot provide an adequate prediction of the behavior of nanomaterials. The ongoing revolution of the nanotechnology has imposed significant impact into biomedical research and engineering applications. The possible environmental and health effects of nanoparticles have raised concerns about the toxicity of nanomaterials as a vital issue for the evaluation of their application [12-15].

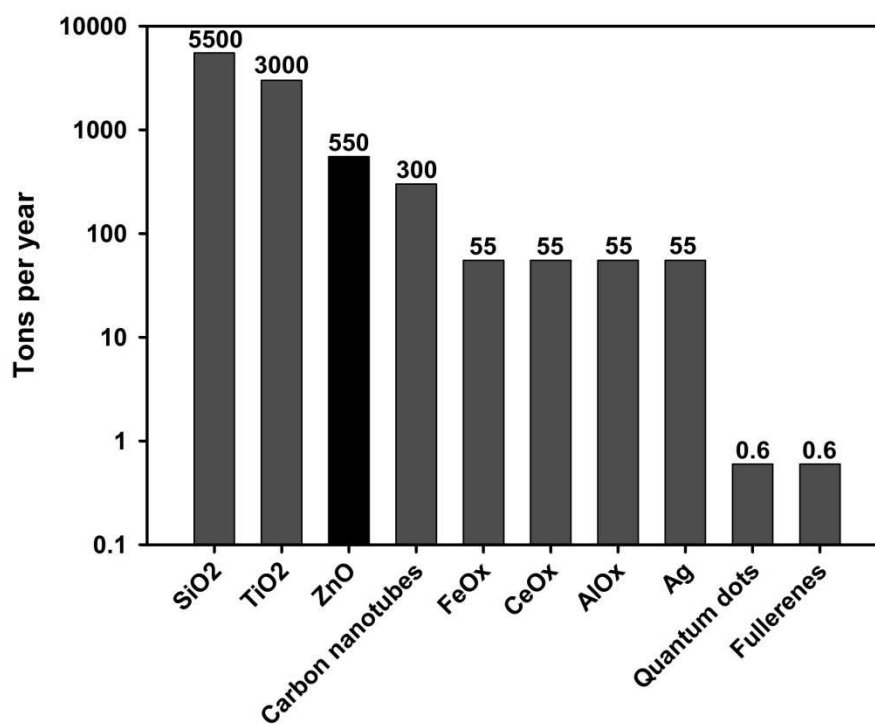


Figure 1.1: Annual production volumes of nanomaterials. Reference [3]

1.2 ZnO powder

In 14th century, zinc was firstly known as a metal in Zewar, India. Zinc oxide (ZnO) was produced through the smelting process [16]. In the ancient time, ZnO was used as a paint or medicinal ointment for the treatment of carbuncles and boils

[17]. The implement of ZnO in skin lotions has sustained up to the present day. The mixtures of zinc and iron oxide were named as calamine lotion [18]. Nowadays, ZnO has been utilized for more medicinal purposes, such as baby powder and cream, anti-dandruff shampoos and antiseptic ointment [19].

ZnO attracted much attention from researchers and it became one of the first materials being studied since 1935. The first scanning-transmission electron microscopy picture of a ZnO crystal was taken in 1938 [20]. In the nineteenth century, two large-scale processes, namely indirect (French) process and direct (American) process were designed to synthesis ZnO. Until now, the largest amount of ZnO is produced by indirect process [21]. This process was developed between 1840 and 1850 to fulfill the demand of use in paints.

The French process is considered as the fastest and most dynamic industrial method in producing ZnO [22]. Zinc metal is heated in the furnace crucible until it melts and vaporizes. When the zinc vapor exited the crucible, it is oxidized into ZnO, which was transported through a 100-150 m long cooling duct. The zinc vapor has a nozzle speed of $8-12 \text{ ms}^{-1}$ causing rapid oxidation at a temperature of $1100-1400 \text{ }^\circ\text{C}$. Multiple morphological structures can be obtained from the oxidation process, including rods, plates, boxes and mallets [22-23]. For the production of “gold seal” or pharmaceutical grade ZnO, special high grade zinc ingot (purity=99.99%) is used whereas ordinary high grade zinc (purity=99.95%) is chosen to produce the ZnO applied in rubber industry [24].

Human has utilized ZnO in multiple applications for thousands of years [25]. It is a well-engineered material with yearly production of about one and a half

million tons [26]. Nonetheless, there are significant new interest from broad areas as the amount of research publications remains rising recently. Besides, there were extensive patent literatures on ZnO which emphasized on large scale industrial manufacture and commercial applications of ZnO [24].

ZnO has been recognized to have three major advantages. Firstly, it is a semiconductor that has direct and wide bandgap of 3.37 eV and it has large excitation binding energy (60 meV). These properties make ZnO an important and useful metal oxide which exhibits near-ultraviolet emission and photonics [27]. Secondly, ZnO is piezoelectric and can be used as electromechanically coupled sensors and transducers. Lastly, ZnO is bio-safe, biocompatible and low in toxicity, which can be used for various biomedical purposes [28]. ZnO is among the five zinc compounds which are generally known as a safe product by the U.S. Food and Drug Administration (21CFR182.8991) [29].

1.3 Skin bacteria

Skin bacteria refer to the bacteria which inhabit on the human skin. There are around 1000 species of skin bacteria on human skin, consisting of 19 phyla [30]. It was estimated that the amount of bacteria on a human is about 10^{12} (1 trillion) [31]. The bacterial survival depends on the exposure of skin to a particular environment and on the native bactericidal behavior in skin.

Typically, skin flora does not impose a pathogenic effect on the skin. Skin allows the growth of commensal bacteria that can fight or compete with the pathogenic bacteria. Environmental conditions, human immunity and organism virulence and adherence are possible causes of skin diseases. Some resident bacteria

not only can cause skin diseases, but even enter the blood circulation system causing the life-threatening infections. For instance, resident gram-positive bacteria include *Staphylococcus*, *Streptococcus*, *Micrococcus* and *Corynebacterium* while gram-negative bacteria consist of *Pasteurella multocida*, *Pseudomonas aeruginosa*, *Capnocytophaga canimorsus*, *Klebsiella rhinoscleromatis*, *Bartonella sp.*, and *Vibrio vulnificus* [32].

Staphylococcus aureus, *Pseudomonas aeruginosa* and *Streptococcus pyogenes* are three common bacteria which potentially can cause diseases to human being. They have different characteristics, such as surface membrane, gram-strain, enzyme production and biological response. Therefore, these three bacteria can be utilized in the antibacterial tests where many other skin bacteria might have similar characteristics and produce comparable bacterial responses as these bacteria.

Generally, skin bacteria present in three regions: sebaceous, moist and dry. Pathogenic skin bacteria cause many skin infections, such as impetigo, folliculitis, furunculosis, carbunculosis, ecthyma, erysipelas, and cellulitis. ZnO is a metal oxide which can effectively kill or inhibit the skin bacteria. It is known to cure many kinds of skin diseases and is widely used in health care products and cosmetics.

Inorganic metal oxides are increasingly used for antibacterial application. The main advantages of using inorganic oxides are their high stability, long shelf life, exhibit strong functional activity and contain mineral elements which are essential to humans. Some of the inorganic oxides that have been tested for antimicrobial activity are TiO₂, ZnO, MgO, CaO, CuO, Al₂O₃, Ag₂O and CeO₂ [33-40]. The

antibacterial activity of ZnO has been studied extensively with different pathogenic and nonpathogenic bacteria such as *S. aureus* and *E. coli* [11, 35].

1.4 Fibroblast cell lines

Fibroblasts are widely distributed in many types of tissues, such as tendon, ligament and skin. Fibroblasts are defined as the cells that produce collagens and they are considered to be the primary source of most extracellular matrix components. Cell lines are useful models for doing research because they provide large amounts of consistent cells for prolonged use. L929 mouse fibroblasts cell lines were used in the cytotoxicity's test in this study due to their consistent and fast growing. These cell lines were suitable to be used to examine the ZnO particles' reaction on them. Several studies had examined the toxicity effect of ZnO on different cell lines, such as human lung epithelial cell [41], T cells [42] and vascular endothelial cells [43].

1.5 Objectives of study

The principal objectives of this research work are elaborated in the following points:

1. To investigate the structural and optoelectronic properties of specific desired ZnO structures.
2. To study the effect of surface modification through annealing process and UVA illumination on the surface properties of ZnO structures.
3. To analyse the antibacterial activities of ZnO structures against *Staphylococcus aureus*, *Pseudomonas aeruginosa* and *Streptococcus pyogenes*.

4. To investigate the toxicity effect of ZnO structures towards normal cell-line and antibacterial properties of synthesized ZnO-calamine lotions.

1.6 Scope of study

The research on ZnO covers a wide areas and investigations. A specific and concise scope is made to direct the experimental, results and discussions presented in this research work.

Firstly, this work focuses on undoped ZnO as main material. The fascinating applications of ZnO have driven this study to expand the uses of pure ZnO. Besides, the respective ZnO samples are specifically synthesized through French process. Focus is given on this gas phase synthesis (dry method) rather than the wet chemical synthesis. Majority of the world's ZnO powder nowadays is manufactured using French process [24], becoming one of the motivations of the research. Moreover, multiple ZnO structures obtained are studied to highlight the uniqueness of this manufacturing process.

Secondly, this research work focuses on the skin bacteria. Three different strains of skin bacteria are given specific interests in order to investigate the antibacterial activities of ZnO samples, those are *Staphylococcus aureus*, *Streptococcus pyogenes*, and *Pseudomonas aeruginosa*. To study the antibacterial response, several experimental tests are to be conducted: microdilution, optical density measurement and scanning electron microscopy. Microdilution method is used to grow and treat the bacteria in 96 well plate while the bacterial inhibition is examined from the optical density measurement. Scanning electron microscopy is used to look into the morphologies of the bacteria after treatment with ZnO samples.

The responses of the selected skin bacteria towards ZnO samples are described along with several proposed mechanisms, including zinc toxicity, reactive oxygen species production, electrostatic effect, and dissolution of zinc ions.

Thirdly, the characterisations of ZnO are limited to physical, optical, electrical, cytotoxicity and antibacterial analyses. In the optical study of ZnO, photoluminescence tests are limited to room-temperature measurements. For UVA photoactivation used in current-voltage, photoresponse, and antibacterial tests, the wavelength and intensity of the UVA light is maintained at 390 nm and 1.8 mW/cm², respectively. In the measurement of antibacterial responses, the antibacterial works are limited on microdilution method while the growth of bacteria is monitored by optical density assessments. The applications of this work focus on the cytotoxicity of pure ZnO (ZnO-Pharma and ZnO-White) samples and calamine lotion preparation from these two ZnO samples. Annealed ZnO-Pharma and ZnO-White samples are excluded from the applications.

1.7 Design of experiment

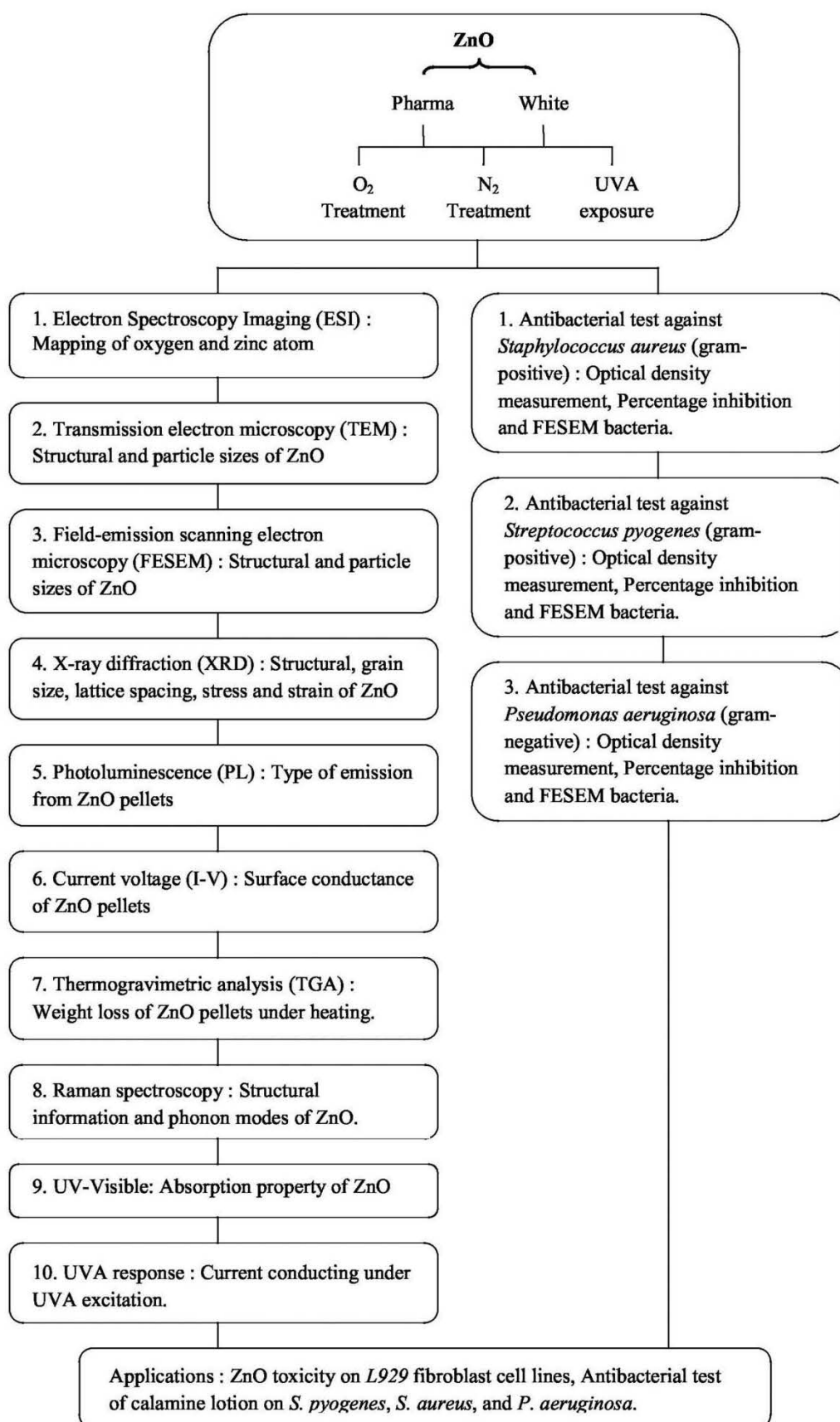


Figure 1.2: Flow chart of experiment.

1.8 Background of study

To date, diverse morphologies of ZnO structures with different dimensional architectures have been investigated such as tubes, belts, wires, rods, plates, rings, tetrapods, combs and flowers [44-47]. Wide applications of ZnO are either dependent upon or are affected by impurities and defects. Furthermore, morphology, particle size, crystal orientation, oxygen defects and crystallinity are among the factors that play important roles in determining the electrical, optical, catalytic, and even antibacterial function of ZnO. The high surface area of nano-scale structures as well as chemical compositions and atomic arrangement at the surface significantly modify their optoelectronic applications. Many annealing parameters such as temperature, duration, atmosphere, and gas pressure can be varied to produce different surface defects on the ZnO structure.

The annealing effects on ZnO thin films have been intensively investigated [48-51]. However, some studies obtained different experimental results. Annealing treatment studies on ZnO powder also remain inconclusive. Further understanding and elucidation are required to study the optoelectronic and surface defect characteristics of ZnO structures under different treatment conditions. The non-stoichiometric chemical component in the samples was revealed to be correlated to the defect formation, particularly oxygen vacancies. More works are required to compare and observe the surface modification of the concentration of oxygen and zinc ions after the ZnO powder samples were annealed in oxygen and inert gas ambient respectively. Changes in the properties were attributed to the surface band bending effect and ratio of oxygen to zinc (O:Zn), which will be discussed in the present study. Furthermore, electron spectroscopy imaging (ESI) assessment was

used to investigate the elemental distributions and surface defects configurations of ZnO powder.

ZnO is known to exhibit antimicrobial activity and has higher stability than organic materials. The release of reactive oxygen species (ROS) especially superoxide anion, hydroxyl radical, hydrogen peroxide, and hydroxyl ion [52, 35] has been documented as possible mechanisms of the antimicrobial behavior of zinc oxide. The nano-sized particles of zinc oxide possess a large surface-to-volume ratio that may exhibit stronger antimicrobial activity. Besides, different structural morphologies of ZnO can exhibit selective antimicrobial responses. Meanwhile, different bacteria strain exhibit various affinities toward ZnO structures depending on bioactivity and bacteria life processes. Therefore, further investigation is required to justify the performance of different ZnO structures toward the targeted microbe. The selective bioactivity of bacteria is due to the different biological structure of the bacteria that may render ZnO to have different effectiveness for antibacterial application. More studies are necessary to determine bacteria response towards ZnO as well as the antibacterial mechanism of ZnO.

Pathogenic skin bacteria cause many skin infections, including impetigo, folliculitis, furunculosis, carbunculosis, ecthyma, erysipelas, and cellulitis. ZnO is known to cure many kinds of skin diseases and is widely used in health products and cosmetics. Moreover, certain morphological structures of ZnO particularly at the nanoscale are believed to show a relatively greater impact in overcoming skin infections. In this work, three types of pathogenic skin bacteria were studied, namely, *S. pyogenes*, *S. aureus*, and *P. aeruginosa*. These three bacteria have different characteristics in the aspects of surface membrane and biological response. The

effect of ZnO samples that have different structural morphologies on selected skin bacteria was investigated. The level of inhibition of each skin bacteria was also discussed to compare the biological reaction of relevant bacteria with ZnO structures.

The motivation of this work is to investigate the effect of different ZnO structures on the antibacterial activity. The correlation of the surface characteristics of ZnO and bacterial inhibition were discovered to explain the possible working mechanisms of ZnO on the antibacterial response. The work has the mission to find out the enhancement method of antibacterial performance and construct suitable corresponding mechanism models.

1.9 Overview of study

In Chapter 2, literature review is made on the properties of ZnO crystalline, including physical, crystallinity, defect formation and energy levels. Surface and lattice defects are given specifically emphasize to look into the atomic arrangement and crystalline orientation of ZnO structures. The theories of surface recombination and surface band bending were also explained.

Besides, reviews are also done on the antibacterial function of ZnO particles. Many works reported the antibacterial results of micro/nano ZnO, but present different level of bacterial inhibition. Moreover, several mechanisms were also proposed from the other researchers to explain how the ZnO particles interact with the bacteria. Three types of skin bacteria are emphasized in this study where the properties of these bacteria are explained explicitly in Chapter 2 as well. The toxicity levels of several synthesized ZnO towards difference cell lines are reviewed based on the other researchers' work.

Chapter 3 explains the experimental details employed in this work. The characterisation of ZnO crystalline was done in Nano-optoelectronic research (NOR) and Technology Laboratory in School of Physics. Electrical, optical, structural and morphology (FESEM) properties were investigated using spectroscopy and microscopy instruments in NOR laboratory whiles the morphology and elemental mapping (TEM and ESI-EFTEM) were studied in electron microscopy laboratory in School of Biology. The antibacterial test was conducted in Microbiology laboratory in School of Medical Sciences (Health campus USM) whiles cyto-toxicity test of ZnO was carried out in Advanced Medical and Dental Institute (AMDI USM). This work involved multi-disciplinary of research which collaborated with other schools in order to implement the prepared materials in biomedical function.

In Chapter 4, all the experimental data and images are presented: FESEM, EFTEM-ESI, TEM, TGA, XRD, PL, I-V, UV-Vis, Raman, optical density of bacteria, and cytotoxicity results. The data are analysed to look into the changes or differences between the ZnO-Pharma and ZnO-White samples in the aspects of physical, chemical composition and antibacterial properties. Chapter 5 provides a detailed discussion on elemental distribution of Zn and O atoms of ZnO structures based on EFTEM-ESI results. The surface defects are explained and correlated with their effects on the structural, optical and electrical properties. Besides, the antibacterial efficacies of ZnO structures are compared and the mechanisms involved in the test are discussed. The toxicity reactions induced by ZnO are explained. Lastly, all the research outputs are concluded in Chapter 6 and future research projects are also recommended.

The significance of this study is the multi-disciplinary research-integration between the physical characterisation in nanotechnology and biofunction of nanomaterial in bio-medical application. This is important not only to discover the new technique in nanotechnology, but also utilize the nanotechnology to characterise and enhanced the properties of biomaterial. In the end of this project, the experimental results are used to produce calamine lotions which have commercial value in market.

CHAPTER 2: LITERATURE REVIEW

2.1 Introduction

The principles and theories of this research are presented in this chapter. In the beginning of the chapter, the applications and several properties (physical, electrical and optical) of ZnO are discussed. Subsequently, type of bacteria strain and bacterial characteristics are addressed. The working principles of toxicities of ZnO towards bacteria are also briefly described in this chapter.

2.2 Application of zinc oxide

ZnO is widely used in our society, and indeed it is an essential element in industrial manufacturing such as paints, toothpastes, beauty products, cosmetics, drug carriers, fillings in medical materials, plastics, rubber, soap, textiles, floor coverings, and industrial coatings [53-60]. With the advancement of synthesis technology of ZnO particles, thin films and single crystals, many ZnO devices have been fabricated. Among the devices include field emission sources, gas and chemical sensors, solar cells, LCDs, UV light emitters, piezoelectric and spintronic devices [61-67].

The revolution of existing technologies with ZnO nanoparticles has led to the development of improved sunscreens, cosmetics, coatings, pharmaceuticals and textiles. Due to the remarkable antimicrobial of ZnO nanoparticles, intensive researches have been conducted, and even applied this material on many innovation products [68-70]. Furthermore, ZnO nanoparticles were used as additive in many sunscreen skin lotion, antiseptic cream, talcum and ointment. Anti-UVA and anti-UVB properties make ZnO nanoparticles suitable for UV-protection healthcare.

2.3 Properties of zinc oxide

ZnO melts at 2250 K and belongs to the group of II-VI binary semiconductors. ZnO crystallizes in the wurtzite phase at room conditions which is made of hexagonal close-packed sub-lattices of the anion (oxygen) and cation (zinc) displaced along the [0001] direction. It possesses a hexagonal unit cell that belongs to the C_{6v}^4 space group $P6_3mc$. Every zinc atom in the wurtzite lattice is bounded by sp^3 covalent bonding to four oxygen atoms, which are located in the vertices of a tetrahedron. The Zn-O bond in bulk ZnO exhibits both covalent and ionic character. According to Ermoshin and Veryazov, the Zn-O bond has a Wiberg index W (ZnO) of 0.11e, a zinc valence of 0.47, and a total quantum chemical valence of 2.0 [71]. The orientation of axes and faces in a wurtzite lattice is denoted by four-digit Miller indices $hkil$. The c -axis direction is referred to as [0001], and the surface perpendicular to the c -axis is the hexagonal (0001) plane.

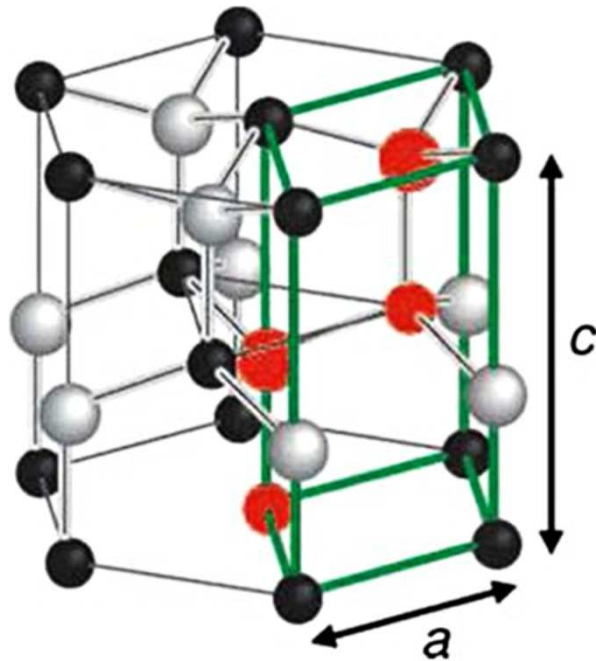


Figure 2.1: Hexagonal wurtzite-type lattice of ZnO crystal structure [72].

Fig. 2.1 shows the crystalline structures of ZnO with atoms of molecular base unit ($2 \times \text{ZnO}$) are marked by red full circles and the primitive unit cell by green lines. The wurtzite lattice consists of three parameters for a hexagonal unit cell: basal plane lattice constant $a=3.2495\text{\AA}$, uniaxial lattice constant $c=5.2069\text{\AA}$ and the internal coordinate $u=3/8$ [73]. The tetrahedral coordination in ZnO crystal produces a non-central symmetric structure which leads to piezoelectricity and pyroelectricity. Besides, ZnO possesses polar surfaces whereby the basal plane is the most common polar surface. Several properties of zinc oxide are summarized in Table 2.1.

Table 2.1: Typical properties of ZnO [73-75].

Properties	Values
Lattice constants (T=300 K): a_0	0.3247 nm
c_0	0.5207 nm
Density	5.606 g/cm ³
Melting point	2248 K
Relative dielectric constant	8.66
Gap Energy	3.37 eV, direct
Intrinsic carrier concentration	$<10^6 \text{ cm}^{-3}$
Exciton binding energy	60 meV
Electron effective mass	0.24
Electron mobility (T=300K)	200 cm ² /Vs
Hole effective mass	0.59
Hole mobility (T=300 K)	5-50 cm ² /Vs
Molar mass	81.408 g/mol
Solubility in water	0.16 mg/100mL
Refractive index	2.004
Stable crystal structure	Wurtzite
Thermal conductivity	0.6-1.1 Wcm ⁻¹ K ⁻¹
Electronic configuration	Zinc : $3d^{10} 4s^2$ Oxygen : $2s^2 2p^4$
Elastic modulus	149-159 GPa
Hardness	8.5-8.9 GPa
Specific heat capacity at constant Pressure, C_p	40.3 Jmol ⁻¹ K ⁻¹

2.4 Electrical property of ZnO

With a large and direct bandgap semiconductor, ZnO attracts much attention for many optoelectronic applications. The advantages of having a large bandgap include high-power and high-temperature operations, lower noise generation, sustain large electric fields, and higher breakdown voltages.

Typically, the background carrier concentration varies according to the quality of the layers but is usually $\sim 10^{16} \text{ cm}^{-3}$. Look *et al.* reported *n*-type doping is $\sim 10^{20}$ electrons cm^{-3} and *p*-type doping is $\sim 10^{19}$ holes cm^{-3} [76]. Due to the exciton binding energy of 60 meV at 300 K, ZnO attracts much attention for optoelectronic device applications. The electron effective mass is $0.24m_0$, and the hole effective mass is $0.59m_0$ [74].

In 1930s, Wagner investigated the effect of crystal stoichiometry on the electrical properties of oxides. Wagner *et al.* [77] showed that the oxygen content of the crystals varied by annealing at different oxygen partial pressures, thereby changes the electrical carrier concentration and the conductivity because of the reaction between oxygen vacancies or interstitial zinc atoms and electrons in the conduction band. It was found that the conductivity of ZnO depends significantly on the stoichiometry, the oxygen or zinc partial pressure during growth or annealing. Fritsch reported the comprehensive measurements of conductivity, Hall effect and thermovoltage on polycrystalline zinc oxide plates, single crystalline ZnO needles and evaporated zinc oxide films [78]. The polycrystalline and ZnO single crystalline needles exhibited resistivities of about 0.2–0.7 Ωcm at room temperature. Annealing at 900°C in oxygen increased the resistivities by about two orders of magnitude. The carrier densities obtained were $1 \times 10^{18} \text{ cm}^{-3}$ for as prepared ZnO plates and 2×10^{16}

cm^{-3} for oxygen annealed samples [78]. Zhang *et al.* [79] reported that annealing at 773 K in air increases the resistivities of ZnO films by about nine orders of magnitude. The absorbed oxygen removes zinc interstitials or oxygen vacancies, thus reducing the density of donor-like defects and the carrier density.

Typically, ZnO crystals are not intentionally doped, whereby intrinsic defects in zinc oxide are due to zinc interstitials or oxygen vacancies. Annealing the crystals in an oxygen atmosphere produced crystals of higher resistivity while annealing in vacuum, under reducing conditions (hydrogen or nitrogen atmosphere) or in zinc vapor produced better conducting samples. Tomlins *et al.* [80] investigated the self-diffusion of zinc in ZnO single crystals with its electrical transport properties. They suggested that zinc diffusion likely controlled by a vacancy mechanism where oxygen vacancies are the intrinsic defects leading to n-type conductivity of zinc oxide. Erhart *et al.* [81] performed density-functional calculations of defect formation energies and diffusion constants in ZnO, in which zinc vacancy and oxygen interstitials were assigned as acceptors while zinc interstitials and oxygen vacancies have energetic shallow donor positions in the band gap.

2.5 Optical property of ZnO

The optical properties of a semiconductor are originated from both intrinsic and extrinsic effects. Intrinsic optical transitions take place between the electrons in the conduction band and holes in the valence band. Extrinsic properties are correlated to dopants or point defects and complexes which normally create electronic states in the bandgap. The presence of impurities can influence both optical absorption and emission processes.

The optical properties and electronic states of the bound excitons of ZnO are strongly influenced by the energy band structure and lattice dynamics. Meyer *et al.* [82] established a comprehensive treatment and analysis of the excitonic spectra obtained from ZnO. Several groups had demonstrated the laser emission from ZnO-based structures which operated at room temperature and had low threshold currents [83-84]. Through alloying with MgO or CdO, the band gap energy of ZnO can be modified to higher or lower values [85-86]. Besides, doping with Al or Ga even can monitor the n-type electrical conductivity of ZnO [87-88]. However, there is lack of data on p-type ZnO as it is still a challenge to obtain a p-type conductivity.

The optical phonons of wurtzite-structure at the Γ -point of the Brillouin zone can be described as following equation [89-90]:

$$\Gamma^{opt} = 1A_1 + 2B_1 + 1E_1 + 2E_2 \quad (2.1)$$

The branches with E_1 - and E_2 -symmetries are twofold degenerated. A_1 - and E_1 -modes are polar modes which can be divided into transverse optical (TO) and longitudinal optical (LO) phonons. The anisotropy is due to the short-range interatomic forces while A_1 - and E_1 -modes possess different frequencies [90].

Both A_1 - and E_1 -modes are Raman and IR active. The two nonpolar E_2 -modes $E_2^{(1)}$ and $E_2^{(2)}$ are Raman active only. The B_1 -modes are IR and Raman inactive (silent modes). Thoma *et al.* [91] and Hewat [92] reported phonon dispersion curves of wurtzite-structure and rocksalt-structure ZnO throughout the Brillouin zone. Table 2.2 lists down the phonon mode of ZnO bulk and thin film samples which were obtained by Raman scattering spectroscopy.

Table 2.2: Optical phonon modes of ZnO bulk and thin films samples through Raman spectroscopy.

References	$E_2^{(1)}$ (cm^{-1})	$A_1(\text{TO})$ (cm^{-1})	$E_1(\text{TO})$ (cm^{-1})	$E_2^{(2)}$ (cm^{-1})	$A_1(\text{LO})$ (cm^{-1})	$E_1(\text{LO})$ (cm^{-1})
Arguello [93]	101	380	413	444	579	591
Calleja [94]	98	378.5	410	438	-	590
Decremps [95]	99	382	414	439	574	580

In Raman spectra of ZnO micro- or nano-structures, two possible mechanisms for the phonon peak shifts are identified. Firstly, it is due to the spatial confinement within the nanocrystal or quantum dot boundaries. Secondly, it relates to the phonon localization by defects. Normally, nano-sized crystals or quantum dots produced by chemical methods or by the molecular-beam epitaxy tend to have more defects compared to bulk crystals. Richter *et al.* [96] investigated the spatial confinement of optical phonons and found that the Raman spectra of nanocrystalline semiconductors are redshifted and broadened due to the relaxation of the q -vector selection rule in the finite size nanocrystals. Optical-phonon confinement in wurtzite nanocrystals results in slightly changes in Raman spectra because of the optical anisotropy of wurtzite lattice. In addition, Fonoberov and Balandin [97-99] derived analytically an expression for the interface and confined polar optical phonon modes in spheroidal quantum dots (QDs) which has wurtzite crystal structure. Their work showed that confined optical phonons in wurtzite nanocrystals have a discrete spectrum of frequencies different from those of bulk phonons.

At room temperature, the photoluminescence (PL) spectrum of a typical ZnO normally exhibits two types of emissions: a UV emission band and a broad visible emission band. The UV emission band is correlated to a band-edge transition of ZnO or excitonic recombination while the broad visible emission band located from 420 nm to 700 nm is known as deep level emission band (DLE). Several works had

reported the origin of the DLE. The DLE band has been reported to be ascribed to some defects in the crystal structures, such as oxygen vacancies (V_o), zinc vacancies (V_{zn}), oxygen interstitial (O_i) and zinc interstitial (Zn_i) [100-105].

There are two recombination mechanisms in semiconductors, namely radiative recombination and non-radiative recombination. In radiative recombination, one photon was emitted with energy equal to or approximate to the bandgap energy of the semiconductor, as illustrated in Fig. 2.2. Recombination of a free electron and a hole result in photon emission from direct bandgap ZnO.

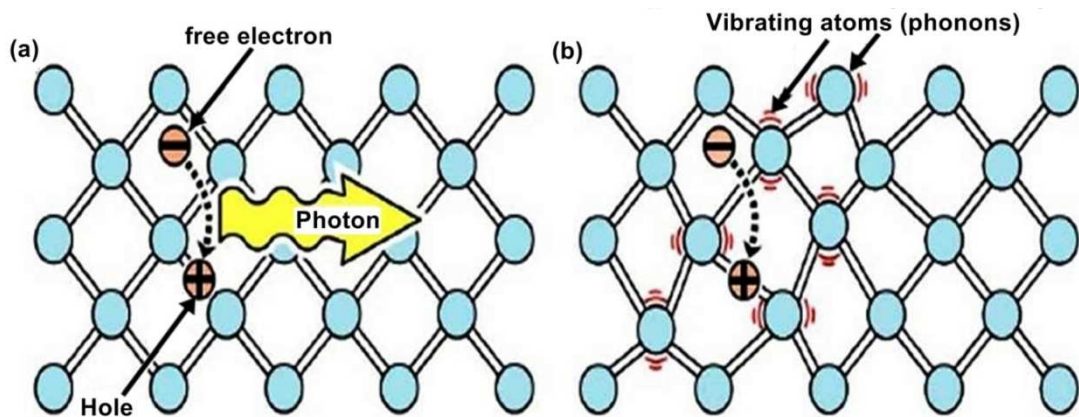


Figure 2.2: (a) Radiative recombination; (b) Non-radiative recombination [106].

Non-radiative recombination can occur in three physical mechanisms, i.e. (1) non-radiative through deep level energy transition; (2) Auger recombination; (3) surface recombination. Fig. 2.3 illustrates the mechanisms of non-radiative via deep level energy transition and Auger recombination.

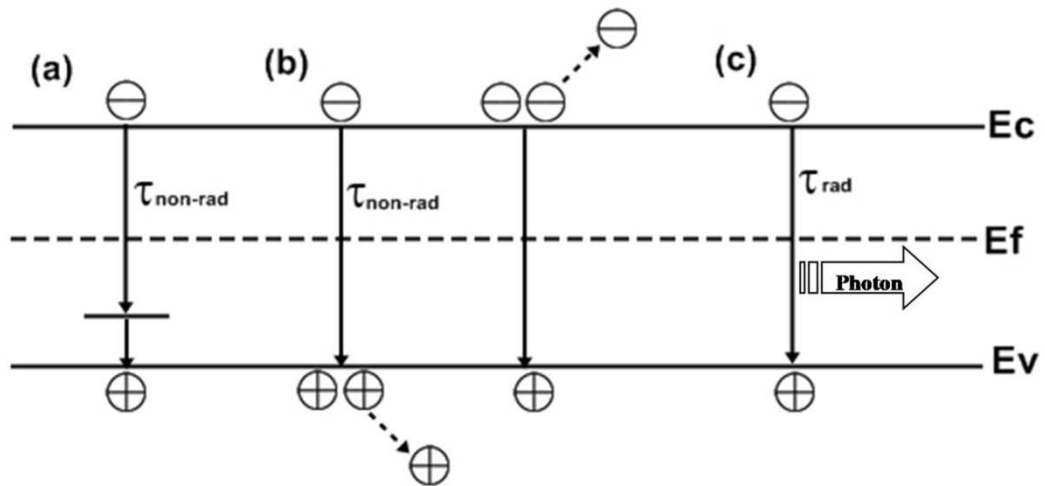


Figure 2.3: Band transitions in a semiconductor: (a) non-radiative via deep level; (b) non-radiative via Auger process; (c) radiative with a photon emission. [107]

2.5.1 Non-radiative via deep level energy

Non-radiative recombination is normally originated from the defects in the crystal structure, such as impurities, native defects, dislocations, and other complexes of defects. Native defects include interstitials, vacancies and antisite defects which form one or few energy levels within the forbidden gap of the semiconductor. For ZnO, the calculated defect energy levels were illustrated in Fig. 2.4 based on several literature sources. The donor defects are $Zn_i^{••}$, Zn_i^{\bullet} , Zn_i^x , $V_o^{••}$, V_o^{\bullet} , V_o and the acceptor defects are V_{Zn}'' , V_{Zn}' . These levels lead to radiative or non-radiative recombination. Energy levels within the gap of the semiconductor form recombination centers which act as shallow or deep level energy.

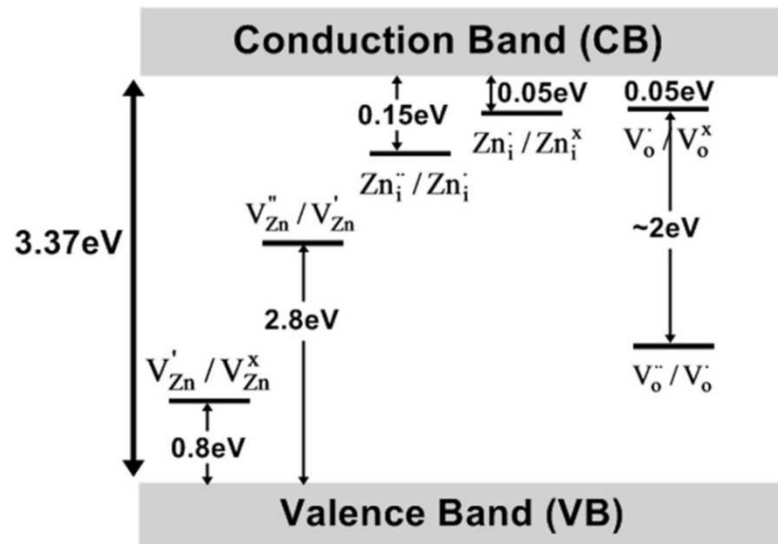


Figure 2.4: Energy levels of native defects in ZnO. [108]

Deep levels in the forbidden energy gap of semiconductor essentially act as carrier recombination or trapping centers and adversely affect device performance. Native defects in the lattice can give rise to deep levels in semiconductor. The excess energy of carriers recombining at these levels is carried away by single or multiple phonon, whereby they were known as “killed centers” [109].

2.5.2 Auger recombination

Fig. 2.3(b) shows the Auger recombination process, which can become important in direct bandgap materials. The Auger recombination process is a non-radiative process. There are two case of Auger recombination: (i) recombination between an electron and hole, accompanied by the transfer of energy to another free hole; (ii) recombination between an electron and hole can result in the transfer of energy to a free electron. Without moving to another energy band, the energy is passed to a third carrier, which experiences an excitation to a higher energy level. The third carrier will subsequently lose its excess energy to thermal vibrations. Such